Journal of Invertebrate Pathology 99 (2008) 302–311

Contents lists available at ScienceDirect

Journal of Invertebrate Pathology

journal homepage: www.elsevier.com/locate/yjipa

Molecular and ultrastructural characterization of *Andreanna caspii* n. gen., n. sp. (Microsporida: Amblyosporidae), a parasite of *Ochlerotatus caspius* (Diptera: Culicidae)

Anastasia V. Simakova [a], Charles R. Vossbrinck [b], Theodore G. Andreadis [b,*]

[a] *Tomsk State University, Lenina Street, 32, Tomsk 634050, Russia*
[b] *The Connecticut Agricultural Experiment Station, 123 Huntington Street, New Haven, CT 06511, USA*

ARTICLE INFO

Article history:
Received 13 May 2008
Accepted 18 July 2008
Available online 25 July 2008

Keywords:
Andreanna caspii
Microsporidia
Molecular phylogeny
Ultrastructure
Ochlerotatus caspius
Mosquito

ABSTRACT

A new genus and species of microsporidia, *Andreanna caspii* n. gen., n. sp. is described from the mosquito, *Ochlerotatus caspius* (Pallas) based on ultrastructural morphology, developmental characteristics, and comparative sequence analyses of the small subunit (SSU) ribosomal DNA (rDNA). Parasite development is confined to fat body tissue and infected larvae appear swollen with dull white masses within the thorax and abdomen. Meronts have diplokaryotic nuclei and are delineated by a simple plasmalemma contiguous with the host cell cytoplasm. Merogony occurs by synchronous binary division followed by cytokinesis. Diplokaryotic sporonts undergo meiosis and synchronous nuclear division forming sporogonial plasmodia with two, four and eight nuclei enclosed within a persistent sporophorous vesicle. Cytokinesis of sporogonial plasmodia results in the formation of eight uninucleate spores. The episporontal space of early sporonts is filled with a homogeneous accumulation of electron dense granular inclusions and ovoid vesicles of various dimensions, transforming into an interwoven matrix during the initial phase of sporogenesis. Spores are oval, uninucleate and measure 4.8 ± 0.3 × 3.1 ± 0.4 μm (fixed). The spore wall is 260 μm thick with an irregular exospore consisting of two layers (150–170 μm) and a thinner endospore (90–100 μm). The anchoring disk is well developed and is contiguous with a lamellar polaroplast that occupies the anterior third of the spore and possess more narrow lamellae on the posterior end. The polar filament is gradually tapered and arranged in a single row consisting of six coils ranging from 180 to 150 μm in diameter. The posterior vacuole (posterosome) is moderately sized and filled with a matrix of moderate electron density. Phylogenetic analysis of SSU rDNA from *A. caspii* and 30 other species of microsporidia including 11 genera parasitic in mosquitoes using maximum parsimony, neighbor joining and maximum likelihood methods showed *A. caspii* to be a sister group to the clade containing all of the *Amblyospora* species, including *Culicospora, Edhazardia* and *Intrapredatorus*, as well as *Culicosporella* and *Hyalinocysta* thus providing strong support for establishment of *Andreanna* as a separate genus.

1. Introduction

Microsporidia are among the largest and most diverse group of parasitic microorganisms which infect mosquito populations in nature. At present, approximately 150 different species representing 23 genera have been described, 15 of which are monotypic (only one species is known) (Andreadis, 2007). Generic classifications within this group have traditionally been based on developmental cycles associated with merogony (vegetative reproduction) and sporogony (production of spores), nuclear organization, and morphology and fine structure of developmental stages and spores (Larsson, 1986, 1988, 1999; Sprague et al., 1992; Canning and Vavra, 2000). More recently, small subunit ribosomal DNA (SSU rDNA) sequence data have been used to validate new genera and species and determine their phylogenetic placement (Nilsen and Chen, 2001; Andreadis and Vossbrinck, 2002; Vossbrinck et al., 2004; Franzen et al., 2006). Unfortunately, gene sequences have been conducted on fewer than half of the described genera infecting mosquitoes.

While conducting a survey of temporary vernal pool habitats in the Tomsk region of Siberia in Russia, several larvae of *Ochlerotatus caspius* (Pallas) were discovered with patent infections of a novel microsporidium. In this investigation we describe the ultrastructural morphology of all stages of development of the microsporidium in the mosquito host, and further examine SSU rDNA sequence data to determine its phylogenetic placement among other mosquito–parasitic microsporidia. Based on morphological,

* Corresponding author. Fax: +1 203 974 8502.
E-mail address: theodore.andreadis@po.state.ct.us (T.G. Andreadis).

0022-2011/$ - see front matter © 2008 Elsevier Inc. All rights reserved.
doi:10.1016/j.jip.2008.07.004

developmental and comparative rDNA sequence analyses, we propose the creation of a new genus, *Andreanna*, with *Andreanna caspii* as the type species.

2. Materials and methods

2.1. Field collection and host identification

Third and fourth instar *Oc. caspius* larvae infected with microsporidia were collected on June 10, 2006 from a temporary vernal pool located near the village of Teguldet, in the Tomsk region of Siberia, Russia (57° 18′ 44′ pr N, 88° 9′ 46′ pr W). Larvae were initially identified based on morphological characters and descriptive keys of Gucevich et al. (1970).

Host identity was further confirmed by comparative analysis of the small subunit ribosomal DNA (18S rDNA) sequence with those recorded in GenBank/EMBL using amplification and sequencing primers described in Shepard et al. (2006). Briefly, genomic DNA from *Oc. caspius* was liberated while bead-beating larval specimens for microsporidia analysis wherein an aliquot was used for polymerase chain reaction (PCR) amplification of nuclear 18S rDNA. This was performed using the Taq PCR Core Kit (Qiagen Inc. Valencia CA) according to the manufacturer's protocol with 0.6 μM of primers 28F and 16SendR (see Table 2, Shepard et al., 2006). PCR reactions were performed in a thermal cycler (PTC-200 DNA Engine, M.J. Research, Watertown, MA) under the following conditions: 94 °C for 3 min followed by 35 cycles of 94 °C for 45 s, 45 °C for 30 s, and 72 °C for 1 min 30 s, followed by a final extension at 72 °C for 3 min. The amplified PCR product (approximately 1940 nucleotides in length) was confirmed by standard 1% agarose gel electrophoresis, purified using QIAquick PCR Purification Kit (Qiagen Inc. Valencia, CA) according to the manufacturer's protocol, and submitted for direct nucleotide sequencing. For sequencing reactions, approximately 100 ng of purified 18S rDNA PCR product was combined with 0.6 μM of sequencing primer (see Table 2, Shepard et al., 2006) and sterile water. Sequencing reactions were performed at the W.M. Keck Foundation Biotechnology Resource Laboratory (Yale University, New Haven, CT).

2.2. Light microscopy studies

General characterization of the microsporidium was initially made from microscopic (1000×) examination of Giemsa-stained smears of infected tissues from larvae with patent signs of infection. These were air dried, fixed in methanol (5 min) and stained with a 10% (w/v) Giemsa-stain solution (MiniMed, Berdsk, Russia) (pH 7.4, 10–15 min). Measurements of individual developmental stages associated with merogony and sporogony and mature spores were calculated from examination of stained preparations from three different larvae ($n = 50$) with an ocular micrometer. Thoracic segments from individual larvae were fixed in 70% ethanol for DNA isolation, while abdominal segments from the same specimen were processed for comparative electron microscopy as described below.

2.3. Electron microscopy

Abdominal segments from infected larvae were fixed in a 2.5% (v/v) glutaraldehyde solution buffered in 100 mM Na cacodylate (pH 7.4) for 2.5 h at 4 °C, postfixed in aqueous 1% (w/v) OsO_4 (pH 7.4) for 2 h at room temperature, dehydrated through a graded ethanol and acetone series and embedded in Epon 812-Araldite (Fluka, Switzerland). Thin sections (60–100 nm) were stained with 2% (w/v) uranyl acetate in 50% ethanol followed by Reynold's lead citrate and examined in a JEM-100 CX II electron microscope at an accelerating voltage of 80 kV.

2.4. Molecular phylogenetic analysis

Nucleotide sequences were obtained from mature spores that were procured from the thoraxes of naturally-infected fourth instar *Oc. caspius*. Methods were similar to those previously published (Vossbrinck et al., 1998). Whole thoracic segments initially fixed in 70% ethanol were exchanged several times with water and left overnight to rehydrate. The larval material was then homogenized briefly in 500 μl of sterile water, filtered through a 41 μm nylon mesh into a clean 1.5 ml microcentrifuge tube centrifuged and spun at 14,000g for 1 min. The supernatant was removed and 500 μl of sterile water was added. The samples were mixed and allowed to sit for 10–15 min to ensure any residual ethanol was removed from the spores. This process was repeated two to three times. Following hydration, samples were centrifuged at 14,000g for 2 min. The supernatant was removed, and 150 μl of STE buffer (0.1 M NaCl, 10 mM Tris–HCl, 1 mM EDTA, pH 8.0) was added to the spore pellet (Fluka, Buchs, Switzerland), resuspended and placed in a 0.5 ml microcentrifuge tube. A 10 μl aliquot of each sample was then removed and examined by phase contrast microscopy (100×) for the presence of spores. One hundred fifty milligrams of glass beads (212–300 μm diameter) (Sigma, St. Louis, MO) was then added and the tube was shaken in a Mini-Beadbeater (Biospec Products Bartlesville, OK) for 50 s to fracture the spores. The samples were spun briefly and 10 μl was removed to verify spore disruption. The samples were incubated at 95 °C for 5 min, and then centrifuged at 14,000g for 5 min. The supernatant was removed to a clean 1.5 ml microcentrifuge tube and was frozen at −20 °C until use in PCR.

One to 5 μl of the STE-ruptured spore solution was used in a standard PCR reaction (94 °C for 3 min, followed by 35 cycles of 94 °C for 45 s, 45 °C for 30 s, and 72 °C for 1 min 30 s) using primers 18f and 1492r (see below). The PCR product was then purified on a Qiaquick PCR purification kit (Qiagen Company, CA) and prepared for automated sequencing at the Keck Biotechnology Resource Laboratory at Yale University with the following microsporidian primers: 18f, CACCAGGTTGATTCTGCC; SS350f, CCAAGGAYGGCAGCA GGCGCGAAA; SS350r, TTTCGCGCCTGCTGCCRTCCTTG; SS530f, GTG CCAGCMGCCGCGG; SS530r, CCGCGGKGCTGGCAC; 1047r, AAC GGCCATGCACCAC; 1061f, GGTGGTGCATGGCCG; 1492r, GGTTA CCTTGTTACGACTT.

Sequences were obtained from the NCBI GenBank database and were aligned using the ClustalX program (Thompson et al., 1997). Aligned sequences were analyzed by Maximum Parsimony, Maximum Likelihood and Neighbor Joining analyses using PAUP version 3.1b (Swofford, 1998). Bootstrap analysis was accomplished using 1000 Neighbor-joining replicates. Maximum Parsimony analysis was done using the heuristic search method. All characters were unordered and had equal weight, no topological constraints were enforced and 838 characters were parsimony informative. Maximum Likelihood analysis was accomplished using the heuristic search method. The substitution model was selected and the Ti/tv ration was set to two. We selected four microsporidian outgroups: *Nadelspora canceri* from a decapod crustacean, *Vairimorpha necatrix* from a lepidopteran, and *Anncaliia algerae* and *Vavraia culicis* from dipterans (mosquitoes) representing a diversity of microsporidia from clades 3 and 4 of Vossbrinck and Debrunner-Vossbrinck (2005). Additional species included in the phylogenetic analyses are shown in Table 1.

Table 1
Hosts and GenBank Accession numbers for the SSU rDNA sequences of 30 microsporidian species used in the phylogenetic analyses and *Andreanna caspii* n. gen., n. sp. obtained in this study

Microsporidium	Host	Accession No.
Amblyospora californica	*Culex tarsalis* Insecta, Diptera, Culicidae	U68473
Amblyospora canadensis	*Ochlerotatus canadensis* Insecta, Diptera, Culicidae	AY090056
Amblyospora cinerei	*Aedes cinereus* Insecta, Diptera, Culicidae	AY090057
Amblyospora connecticus	*Ochlerotatus cantator* Insecta, Diptera, Culicidae	AF025685
Amblyospora criniferis	*Ochlerotatus crinifer* Insecta, Diptera, Culicidae	AY090061
Amblyospora excrucii	*Ochlerotatus excrucians* Insecta, Diptera, Culicidae	AY090043
Amblyospora ferocis	*Psorophora ferox* Insecta, Diptera, Culicidae	AY090062
Amblyospora indicola	*Culex sitiens* Insecta, Diptera, Culicidae	AY090051
Amblyospora khaliulini	*Ochlerotatus communis* Insecta, Diptera, Culicidae	AY090045
Amblyospora opacita	*Culex territans* Insecta, Diptera, Culicidae	AY090052
Amblyospora salinaria	*Culex salinarius* Insecta, Diptera, Culicidae	U68474
Amblyospora stictici	*Ochlerotatus sticticus* Insecta, Diptera, Culicidae	AY090049
Amblyospora stimuli	*Ochlerotatus stimulans* Insecta, Diptera, Culicidae	AF027685
Amblyospora weiseri	*Ochlerotatus cantans* Insecta, Diptera, Culicidae	AY090048
Amblyospora sp. 1	*Culex nigripalpus* Insecta, Diptera, Culicidae	AY090053
Amblyospora sp. 2	*Cyclops strenus* Maxillopoda, Cyclopoida, Cyclopidae	AY090055
Andreanna caspii	*Ochlerotatus caspius* Insecta, Diptera, Culicidae	EU700339
Anncaliia algerae	*Anopheles stephensi* Insecta, Diptera, Culicidae	AF069063
Culicospora magna	*Culex restuans* Insecta, Diptera, Culicidae	AY326269
Culicosporella lunata	*Culex pilosis* Insecta, Diptera, Culicidae	AF027683
Edhazardia aedis	*Aedes aegypti* Insecta, Diptera, Culicidae	AF027684
Hazardia milleri	*Culex quinquefasiatus* Insecta, Diptera, Culicidae	AY090067
Hazardia sp.	*Anopheles crucians* Insecta, Diptera, Culicidae	AY090066
Hyalinocysta chapmani	*Culiseta melanura* Insecta, Diptera, Culicidae	AF483837
Intrapredatorus barri	*Culex fuscanus* Insecta, Diptera, Culicidae	AY013359
Nadelspora canceri	*Cancer magister* Malacostraca, Decapoda, Cancridae	AY958070
Parathelohania anophelis	*Anopheles quadrimaculatus* Insecta, Diptera, Culicidae	AF027682
Parathelohania obesa	*Anopheles crucians* Insecta, Diptera, Culicidae	AY09006
Senoma globulifera	*Anopheles messeae* Insecta, Diptera, Culicidae	DQ641245
Vairimorpha necatrix	*Pseudaletia unipunctata* Insecta, Lepidoptera, Noctuidae	Y00266
Vavraia culicis	*Culex pipiens* Insecta, Diptera, Culicidae	AJ252961

3. Results

3.1. Host identification

Sequencing of the SSU rDNA fragment from *Oc. caspius* generated a sequence of 1940 nucleotides (GenBank Accession No. EU700339). A comparison with 18 s rDNA sequences of Culicidae species found in GenBank-EMBL initially revealed three nucleotide differences with a sequence derived from *Oc. caspius* collected in Spain (GenBank Accession No. AM071383). However, reexamination of the sequence of *Oc. caspius* from Spain revealed an apparent mistake in the sequence at positions 654 and 655 and we identified one polymorphic nucleotide (position 1455) in our isolate of *Oc. capspius* from Russia, therein demonstrating 100% similarity between the two isolates.

3.2. Gross pathology and prevalence

Microsporidian development was confined to fat body tissue and infected larvae appeared swollen with dull white masses within the thorax and abdomen. The prevalence rate of infection was low and was estimated to be approximately 0.5% ($n = 1222$). Infected larvae were detected in June coincident with mass pupation and adult emergence of the presumably uninfected portion of the *Oc. caspius* population. No attempt was made to examine adults for infection. Associated larval mosquitoes included *Ochlerotatus cantans* (Meigen) and *Ochlerotatus flavescens* (Muller).

3.3. Light microscopy

In Giemsa-stained smears meronts appeared as rounded cells (9.7×9.7 μm) with brightly stained diplokaryotic nuclei. Stages with two diplokaryotic nuclei, also presumed to be meronts, were occasionally observed. Early sporonts were identified by possession of a less intensely stained cytoplasm and were either uninucleate (9.6×9.7 μm) or binucleate (8.1×11.3 μm). Sporogony appeared to occur by synchronous nuclear division forming quadrinucleate and octonucleate stages, and ultimately eight sporoblasts within a persistent sporophorous vesicle (12.9×12.8 μm). Mature spores were uninucleate, oval in shape, and measured $4.8 \pm 0.3 \times 3.1 \pm 0.4$ μm (Fig. 1).

3.4. Ultrastructure

Meronts were delineated by a simple plasmalemma contiguous with the host cell cytoplasm (Fig. 2). They were diplokaryotic with each member of the diplokaryon enclosed within a distinct unit membrane. The cytoplasm was rich in free ribosomes but with weakly developed endoplasmic reticulum. Spindle plaques and associated polar vesicles were occasionally observed adjacent to the nuclei. Merogonial stages with multiple nuclei in the diplokaryotic arrangement and discernible endoplasmic reticulum were seen undergoing synchronous binary division followed by

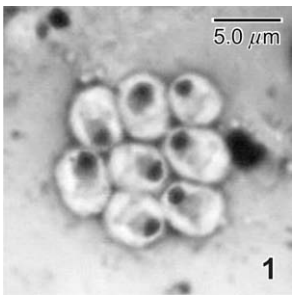

Fig. 1. Sporophorous vesicle with mature spores of *Andreanna caspii* n. gen., n. sp. from a methanol fixed and Giemsa-stained smear.

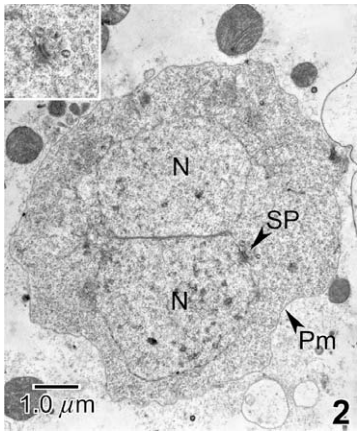

Fig. 2. Merogony in *Andreanna caspii* n. gen., n. sp. Diplokaryotic meront. Inset, higher magnification of spindle plaque and associated polar vesicles. N, nucleus; Pm, plasmalemma; SP, spindle plaque.

cytokinesis to form additional diplokaryotic stages (merogony) (Fig. 3). The number of merogonial cycles could not be ascertained.

Early sporonts (Fig. 4) were identified from meronts by the possession of a thin outer envelope surrounding the plasmalemma that appeared to be of parasite origin (sporophorous vesicle), a more vacuolated cytoplasm with prominent rough endoplasmic reticulum throughout, and numerous elements of Golgi apparatus scattered around the nucleus. The nuclei of these stages were no longer in the diplokaryotic arrangement and the respective nuclear membranes were less well defined. Accumulations of electron dense granular inclusions were also observed within the episporontal space separating the plasmalemma and sporophorous vesicle membrane. These inclusions were largely homogeneous but also consisted of ovoid vesicles of various dimensions (Fig. 5). The inclusions were further detected within small membranous vesicles within the sporont cytoplasm that were apparently responsible for transport and secretion of the material (Figs. 5 and 6). At this stage, some of the Golgi elements appeared to lose their connection with the nuclei (Fig. 7). The progressive deposition and accumulation of the granular inclusions within the episporontal space was coincident with a gradual thickening of the plasmalemma (Figs. 6 and 7) that was fully formed in binucleate stages (Fig. 8).

Binucleate sporonts underwent nuclear division wherein spindle plaques and microtubules were apparent (Fig. 9), forming quadrinucleate sporogonial plasmodia with constricted plasmalemmas surrounding each nucleus (Fig. 10). These cells subsequently underwent synchronous nuclear division producing sporogonial plasmodia with eight nuclei (Fig. 11). Cytokinesis of these octonucleated sporonts ensued and resulted in the formation of eight uninucleate sporoblasts contained within the sporophorous vesicle (Fig. 12).

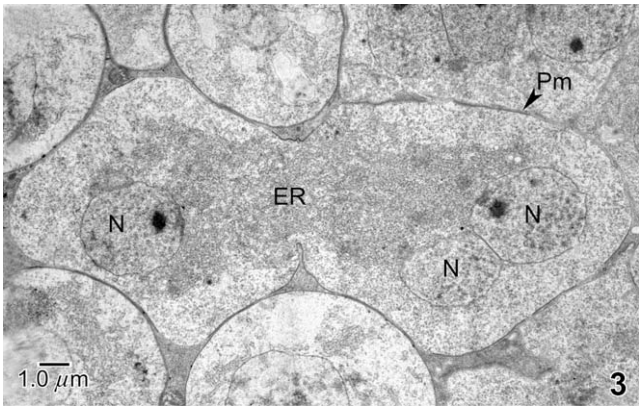

Fig. 3. Merogony in *Andreanna caspii* n. gen., n. sp. Dividing diplokaryotic meront. ER, endoplasmic reticulum; N, nucleus; Pm, plasmalemma; SP, spindle plaque.

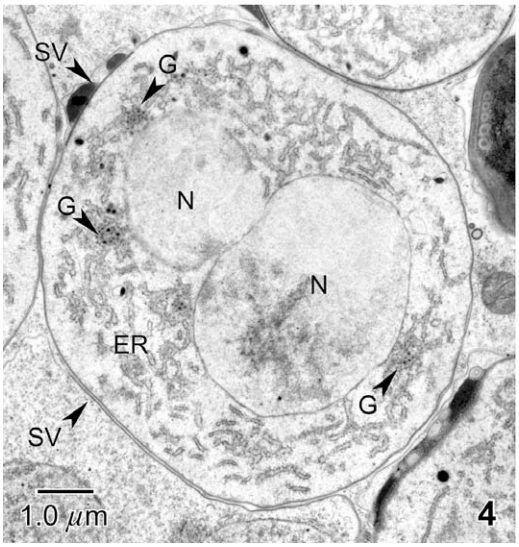

Fig. 4. Early sporogony in *Andreanna caspii* n. gen., n. sp. Early transitional sporont showing Golgi elements (G) located in the vicinity of the nuclear envelops and formation of the sporophorous vesicle (SV). ER, endoplasmic reticulum; N, nucleus.

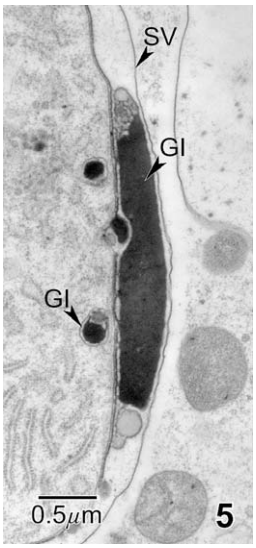

Fig. 5. Early sporogony in *Andreanna caspii* n. gen., n. sp. Higher magnification of early sporonts showing deposition of granular inclusions (GI) within the episporontal space and thickening of the plasmalemma (Pm). SV, sporophorous vesicle.

Early sporogenesis was characterized by differentiation and thickening of the spore wall of each sporoblast. This was coincident with a distinct change in the structure of the granular inclusions within the episporontal space which now appeared as an interwoven matrix (Fig. 13). This was followed by differentiation of the polar filament, polaroplast, posterior vacuole and finally the endospore and exospore wall (Fig. 14). During this phase of sporogenesis the granular matrix of inclusions within the episporontal space gradually disappeared while the membrane of the sporophorous vesicle persisted.

Mature spores were oval and uninucleate (Figs. 15 and 16). The spore wall measured 260 nm in thickness. The exospore was irreg-

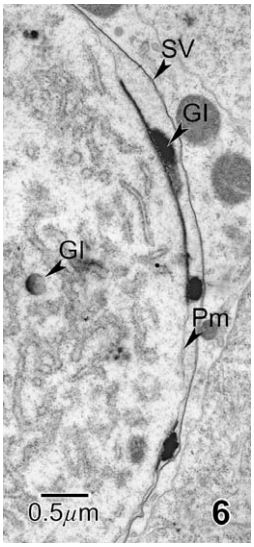

Fig. 6. Early sporogony in *Andreanna caspii* n. gen., n. sp. Higher magnification of early sporonts showing deposition of granular inclusions (GI) within the episporontal space and thickening of the plasmalemma (Pm). SV, sporophorous vesicle.

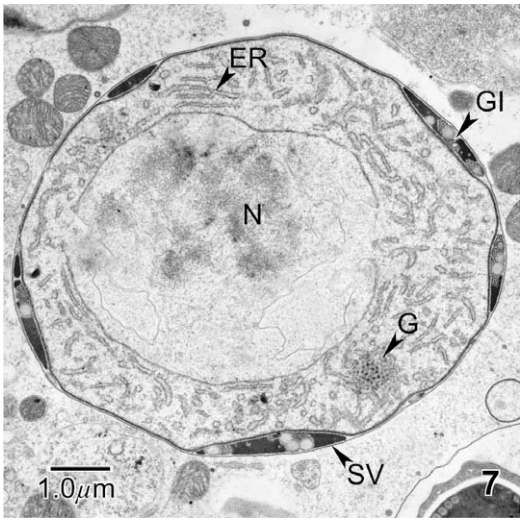

Fig. 7. Early sporogony in *Andreanna caspii* n. gen., n. sp. Cross section through the sporont at a later stage showing complete thickening of the plasmalemma and accumulation of granular inclusions (GI) within the episporontal space. ER, endoplasmic reticulum; G, Golgi; N, nucleus; SV, sporophorous vesicle.

ular, measured 150–170 μm, and consisted of a thin outer layer and a much thicker fibrous inner layer with reduced thickness at the anterior pole. The electron-lucent endospore measured 90–100 μm. The anchoring disk was well developed and was contiguous with a lamellar polaroplast that possessed more narrow lamellae on the posterior end and occupied the anterior third of the spore. The polar filament was gradually tapered being neither of the anisofilar (abruptly constricted) or isofilar type (uniform thickness). It was arranged in a single row and consisted of six coils ranging from 180 to 150 μm in diameter. Spores possessed a moderately sized posterior vacuole (posterosome) that was filled with a matrix of moderate electron density.

3.5. Molecular phylogenetic analysis

Sequencing of the SSU rDNA fragment from the novel microsporidium isolated from *Oc. caspius* generated a sequence of 1262

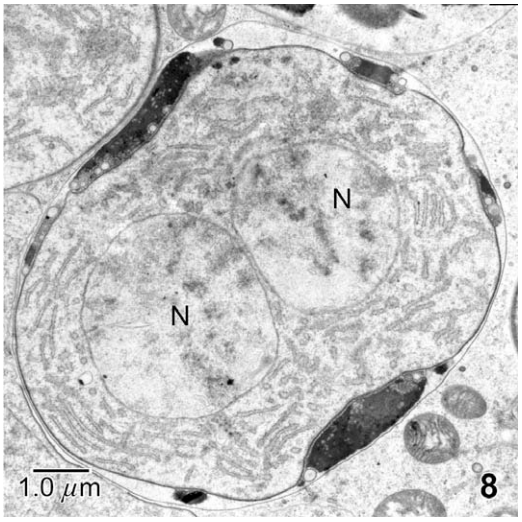

Fig. 8. Early sporogony in *Andreanna caspii* n. gen., n. sp. Binucleate sporont. N, nucleus.

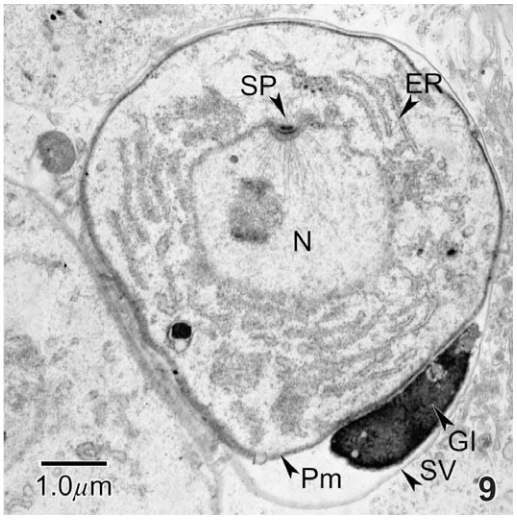

Fig. 9. Late sporogony in *Andreanna caspii* n. gen., n. sp. Dividing sporont nucleus (N). ER, endoplasmic reticulum; GI, Granular inclusions; N, nucleus; Pm, plasmalemma; SP, spindle plaque; SV, sporophorous vesicle.

nucleotides (GenBank Accession No. EU664450). The results of maximum parsimony and bootstrap analyses using the neighbor joining search parameter (1000 replicates) for this isolate and 30 other species of microsporidia are shown in Fig. 17a and b. The placement of the microsporidium from *Oc. caspius* was identical in all analyses including maximum parsimony, neighbor joining and maximum likelihood (data not shown). In each case, this novel microsporidum was the sister group to the clade containing all of the *Amblyospora* species, including *Culicospora magna, Edhazardia aedis* and *Intrapredatorus barri*, and the *Culicosporella* and *Hyalinocysta* species. This entire group formed a sister clade to the *Parathelohania* and *Hazardia/Senoma* clades which are primarily parasites of *Anopheles* mosquitoes (exception *H. milleri*).

Table 2 is a pairwise distance matrix giving the relative differences among selected taxa analyzed in this study. Differences among the *Amblyospora*, *Edhazardia* and *Intrapredatorous* species (10 through 15) ranged from 4.0% to 18.8% (average = 15.3%), while differences between the new microsporidium from *Oc. caspius* and the aforementioned species ranged from 17.0% to 19.2% (average = 18.0%).

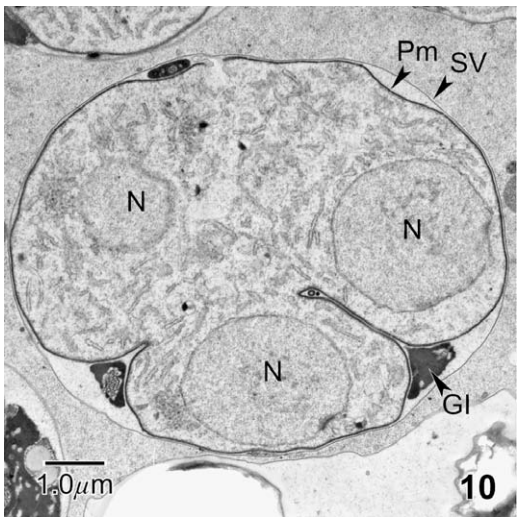

Fig. 10. Late sporogony in *Andreanna caspii* n. gen., n. sp. Section through a quadrinucleate sporogonial plasmodium. GI, Granular inclusions; N, nucleus; Pm, plasmalemma; SV, sporophorous vesicle.

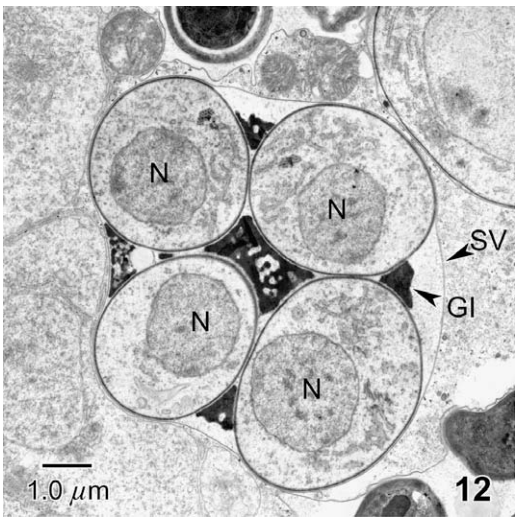

Fig. 12. Late sporogony in *Andreanna caspii* n. gen., n. sp. Early sporoblasts. GI, Granular inclusions; N, nucleus; SV, sporophorous vesicle.

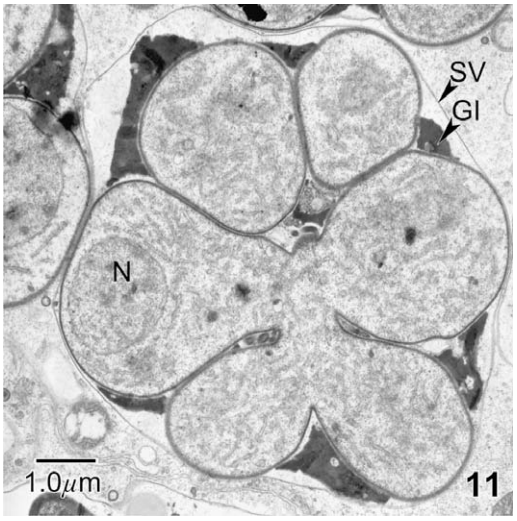

Fig. 11. Late sporogony in *Andreanna caspii* n. gen., n. sp. Section through an octonucleate sporogonial plasmodium. GI, Granular inclusions; N, nucleus; SV, sporophorous vesicle.

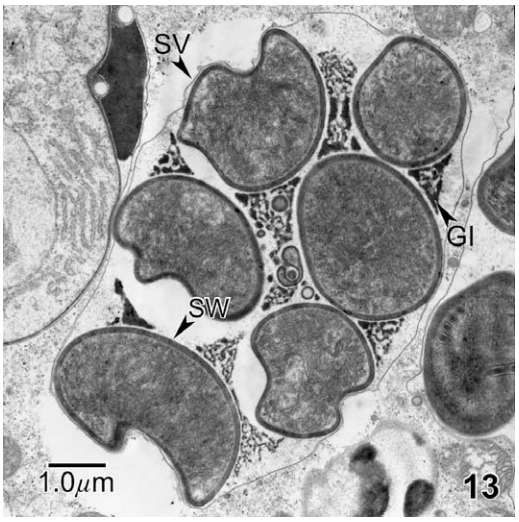

Fig. 13. Sporogenesis and a mature spore of *Andreanna caspii* n. gen., n. sp. Sporoblasts showing formation of the spore wall (SW) with the sporophorous vesicle (SV). Note tube-like structure of the granular inclusions (GI).

4. Discussion

4.1. Morphology and development

The microsporidium described herein from *Oc. caspius* possess many developmental and morphological similarities with *Amblyospora* and other closely related genera. Development in larvae is restricted to fat body tissue and infected fourth instar larvae exhibit nearly identical gross symptoms appearing swollen with white masses of infected tissue within the thorax and abdomen. Meronts are similarly diplokaryotic, have a simple plasmalemma, and develop in direct contact with the host cell cytoplasm. They divide by synchronous binary division during an initial phase of merogony and form binucleate stages. The transition from meront to sporont is characterized by a physical separation of each member of the diplokaryon and a simultaneous formation of a thin-walled sporophorous vesicle. Although we did not observe synaptonemal complexes within the nuclei, these sporonts appear to undergo meiotic division characteristic of the group wherein there is an initial fusion of the two elements of the diplokaryon followed by separation of the chromosomes during meiosis I, resulting in the formation of binucleate sporonts with contracted cell membranes. These subsequently undergo two synchronous divisions (meiosis II and mitosis) to produce a sporogonial plasmodium with eight nuclei.

During the early phases of sporogony there is the typical secretion of metabolic inclusions and accompanying accumulation within the episporontal space separating the plasmalemma and the sporophorous vesicle membrane. However, in addition to granular inclusions, the microsporidium described herein produces a distinct heterogeneous assemblage of uniquely ovoid vesicular-like secretions of various size and electron density (Figs. 5 and 6). These partly resemble secretions observed in *E. aedis* (Becnel et al., 1989, Fig. 45), but are notably distinct from the homogeneous products formed in species of *Amblyospora* (Andreadis and Hall, 1979; Andreadis, 1983; Sweeney et al., 1988; Becnel and Sweeney, 1990; Lukes and Vavra, 1990; Micieli et al., 2000), *Culicosporella*

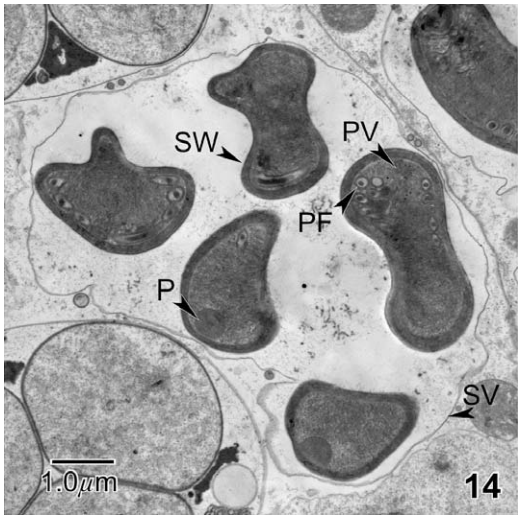

Fig. 14. Sporogenesis and a mature spore of *Andreanna caspii* n. gen., n. sp. Late stage sporoblasts showing differentiation of the polaroplast (P), polar filament (PF), and posterior vacuole (PV). SV, sporophorous vesicle; SW, spore wall.

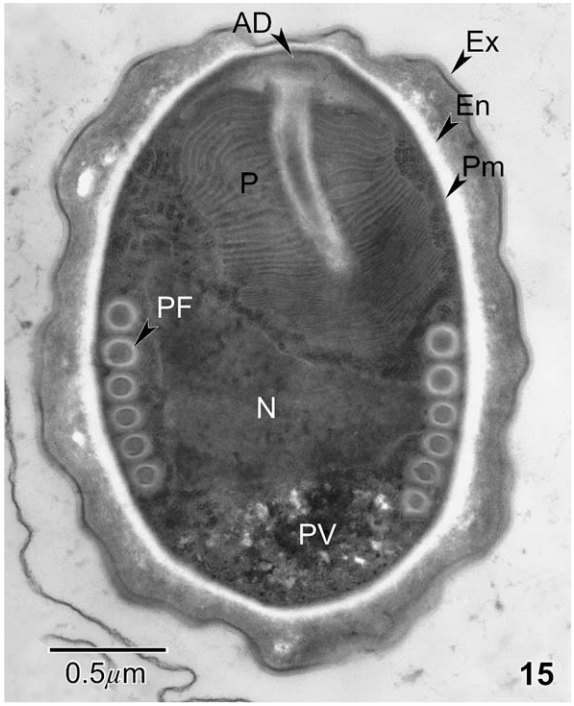

Fig. 15. Sporogenesis and a mature spore of *Andreanna caspii* n. gen., n. sp. Mature spores. AD, anchoring disk; En, endospore; Ex, exospore; N, nucleus; P, polaroplast; PF, polar filament; Pm, plasmalemma; PV, posterior vacuole.

(Becnel and Fukuda, 1991), *Hyalinocysta* (Andreadis and Vossbrinck, 2002), and *Intrapredatorus* (Chen et al., 1998). The change in the structure of the granular inclusions within the episporontal space into a loosely defined interwoven matrix in early sporoblast stages of this new isolate (Fig. 13) also appears to be distinctive, partially resembling the vesicular matrix seen in sporonts of *E. aedis* (Becnel et al., 1989, Figs. 46 and 47), and parallel "sheet-like" secretory products observed in sporoblasts of *Amblyospora trinus* (Becnel and Sweeney, 1990, Fig. 19) and sporonts of *Culicosporella lunata* (Becnel and Fukuda, 1991, Fig. 19). In addition, the prominent tubular extensions of the plasmalemma commonly found in

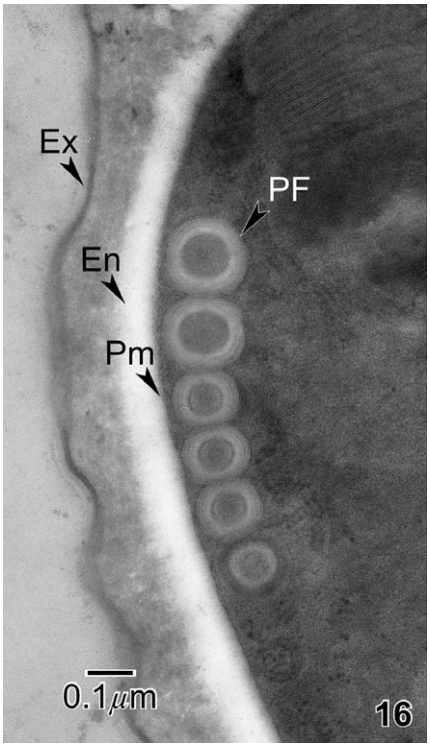

Fig. 16. Sporogenesis and a mature spore of *Andreanna caspii* n. gen., n. sp. Mature spores. En, endospore; Ex, exospore.

sporogonial plasmodia of *Amblyospora* (Andreadis, 1983; Sweeney et al., 1988; Becnel and Sweeney, 1990; Micieli et al., 2000), *Culicosporella* (Becnel and Fukuda, 1991), *Edhazardia* (Becnel et al., 1989), *Hyalinocysta* (Andreadis and Vossbrinck, 2002), and *Intrapredatorus* (Chen et al., 1998) are notably absent in this new microsporidium.

Sporogenesis is unremarkable with a gradual dissolution (reabsorption) of metabolic inclusions within the episporontal space and persistence of the sporophorous vesicle. However, mature spores are morphologically distinct in shape and internal structure from *Amblyospora.* Spores of this novel microsporidium are oval and lack the broadly rounded posterior and narrow anterior ends diagnostic in all species of *Amblyospora* (Sprague et al., 1992; Andreadis, 2007). They also possess a notably reduced posterior vacuole and a tightly compressed lamellate polaroplast in contrast to the bipartite type found in most species of *Amblyospora* in which units of the distal part are somewhat expanded and vesicular in appearance. Most notably, the polar filament is gradually tapered in this microsporidium from *Oc. caspius* in clear difference to the prominent anisofilar types found in meiospores of *Amblyospora*, as well as *Culicosporella*, *Hyalinocysta* and *Intrapredatorus*.

To our knowledge, there are at least three other microsporidia that have been described from *Oc. caspius* for which there are morphological data for comparison with our isolate. Pankova et al. (2000) described a species of *Amblyospora* (*Amblyospora caspius*) from larvae that were also collected from a temporary vernal pool in the Tomsk region of Siberia, Russia. Meiospores of this species were of similar size (4.8 × 3.6 μm), but they were broadly rounded posteriorly, narrowed anteriorly, and displayed a thinner exospore and an anisofilar polar filament with five broad proximal and nine narrow distal coils. Kilochitski (1997, 2002) further described two species of another genus, *Aedispora* (*Aedispora dorsalis* and *Aedispora* sp.) from larvae of *Oc. caspius dorsalis* and *Oc. caspius caspius*, collected in Ukraine. Mature spores of these microsporidia were

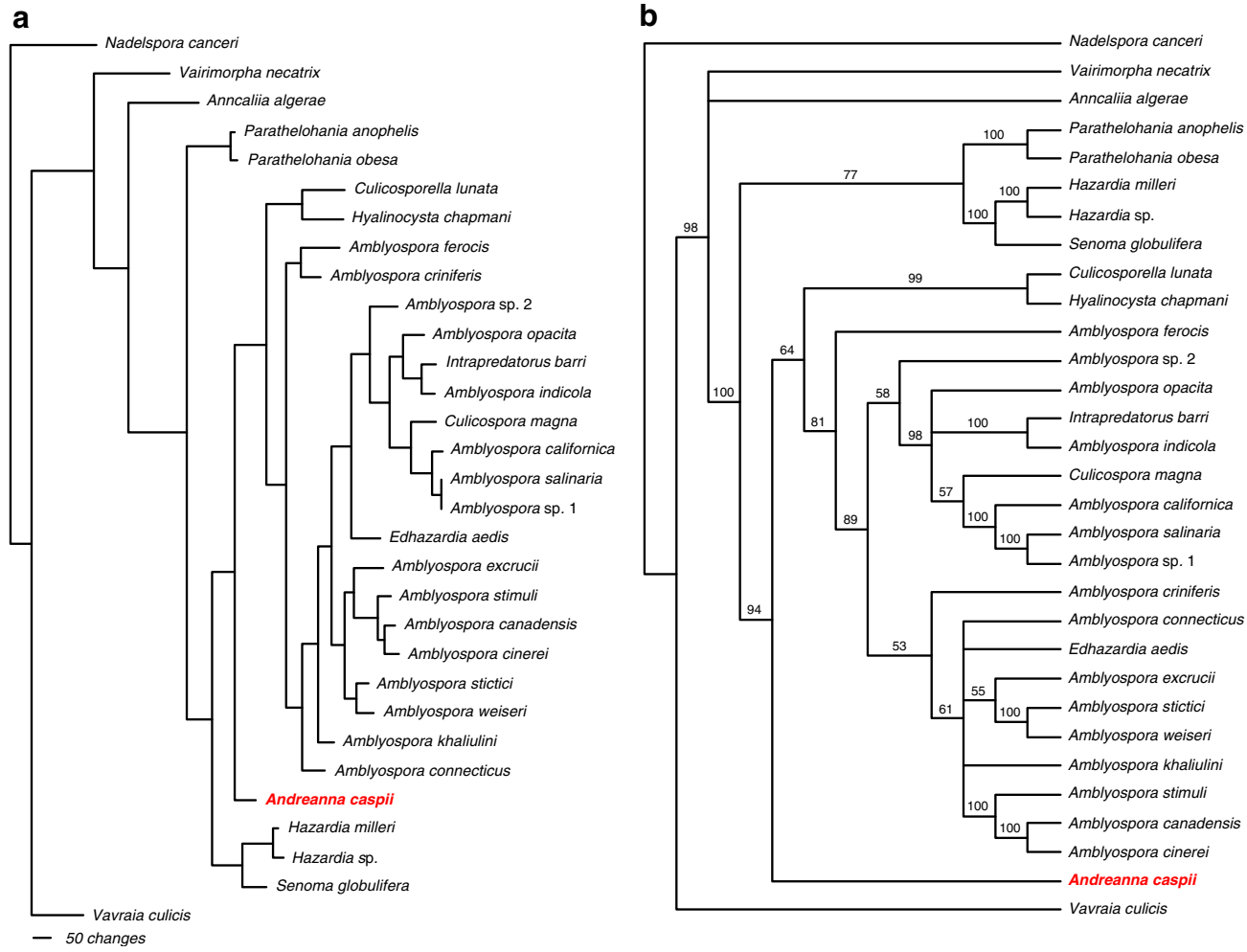

Fig. 17. Phylogenetic trees showing the relationship of *Andreanna caspii* n. gen., n. sp. to 9 closely related genera of mosquito–parasitic microsporidia (including 16 species of *Amblyospora*). Microsporidial outgroups included *Nadelspora canceri* from a decapod crustacean, *Vairimorpha necatrix* from a lepidopteran, and two distally related genera from mosquitoes, *Anncaliia algerae* and *Vavraia culicis*. (a) Cladogram (Maximum Parsimony analysis); (b) Bootstrap analysis based on Neighbor Joining analysis (1000 replicates).

Table 2
Pairwise distance (uncorrected –'p') values observed among rDNA sequences of 11 currently accepted genera of mosquito–parasitic microsporidia, four species of *Amblyospora*, and *Andreanna caspii* n. gen., n. sp. obtained in this study

	1	2	3	4	5	6	7	8	9	10	11	12	13	14
1. ***Andreanna caspii***	–													
2. *Anncallia algerae*	0.340	–												
3. *Vavraia culicis*	0.339	0.359	–											
4. *Culicosporella lunata*	0.237	0.357	0.362	–										
5. *Hyalinocysta chapmani*	0.230	0.350	0.367	0.194	–									
6. *Parathelohania anophelis*	0.214	0.351	0.331	0.272	0.350	–								
7. *Senoma globulifera*	0.185	0.341	0.341	0.279	0.270	0.234	–							
8. *Hazardia milleri*	0.180	0.339	0.322	0.285	0.263	0.222	0.149	–						
9. *Culicospora magna*	0.192	0.372	0.335	0.235	0.219	0.269	0.260	0.220	–					
10. *Edhazardia aedis*	0.178	0.345	0.352	0.230	0.209	0.250	0.238	0.231	0.151	–				
11. *Intrapredatorous barri*	0.178	0.350	0.345	0.228	0.214	0.250	0.234	0.229	0.128	0.145	–			
12. *Amblyospora californica*	0.192	0.348	0.361	0.238	0.227	0.270	0.260	0.237	0.144	0.164	0.152	–		
13. *Amblyospora salinaria*	0.188	0.345	0.355	0.235	0.219	0.267	0.241	0.232	0.140	0.160	0.142	0.040	–	
14. *Amblyospora connecticus*	0.175	0.342	0.351	0.227	0.204	0.243	0.235	0.231	0.156	0.136	0.144	0.184	0.180	–
15. *Amblyospora ferocis*	0.170	0.344	0.343	0.228	0.212	0.249	0.232	0.226	0.167	0.170	0.170	0.188	0.187	0.157

similarly uninucleate and packed in group of eight, but unlike the new species from Siberia, they were elongated and pyriform in shape (10.0–14.5 × 3.5–4.4 μm), possessed a thin (40–60 μm) exospore, a large-chambered vesicular polaroplast, and an anisofilar polar filament with 11–15 coils. Unfortunately, no SSU rDNA sequence data are available from the aforementioned species of

microsporidia for comparative analysis but the morphological differences with this novel isolate from *Oc. caspius* noted above are overtly apparent. It would thus appear that *Oc. caspius* can serve as a host for several species of microsporidia in Siberia and elsewhere in Eastern Europe.

The source of infection in larval stages of *Oc. caspius* could not be determined in the present study and no attempt was made to assess the infectivity of meiospores to larvae. However, considering the site of infection in the host (fat body) and developmental similarity with species of *Amblyospora*, it is logical to infer that these infections were likely derived via transovarial transmission from females infected during the previous spring (*Oc. caspius* is univoltine). Conversely, we can not rule out the possibility that these infections arose from oral ingestion of meiospores, or perhaps from oral ingestion of spores produced in an intermediate host (e.g. copepod) as occurs in *Hyalinocysta* (Andreadis and Vossbrinck, 2002). Efforts are currently underway to examine adult stages of *Oc. caspius* for infection with this microsporidium and identify potential intermediate hosts via laboratory bioassays and comparative rDNA analysis.

4.2. Molecular phylogenetic analysis

The results of our phylogenetic analyses, regardless of the methods employed, provide strong support for establishment of this microsporidium from *Oc. caspius* as a separate genus within clade 1 of Vossbrinck and Debrunner-Vossbrinck (2005) based on current generic designations within the microsporidia. While the two trees generated by Maximum Parsimony and Neighbor Joining Bootstrap analyses differ with respect to the relationships among some *Amblyospora* species, and in the relationships between the *Parathelohania* and *Hazardia/Senoma* clades, this new microsporidium was always seen as a sister taxon to the *Amblyospora* (including *Culicospora, Edhazardia* and *Intrapredatorous*) and *Culicosporella* and *Hyalinocysta* clades. It is logical to assume that the numerous structural, developmental and life cycle similarities between this microsporidium, *Amblyospora*, and related genera, represent pleisomorphic similarities one would expect from a common ancestor thus supporting a growing body of evidence that this entire group of microsporidian parasites of mosquitoes likely arose as a single event.

4.3. Taxonomic summary

Phylum Microspora Sprague, 1977
Class Microsporea Delphy, 1963
Order Microsporida Balbiani, 1882
Family Amblyosporidae Weiser, 1977.

4.3.1. Andreanna n. g

4.3.1.1. Diagnosis. Monotypic genus. Meronts have diplokaryotic nuclei and are delineated by a simple plasmalemma contiguous with the host cell cytoplasm. Merogony by synchronous binary division of diplokaryotic meronts followed by cytokinesis. Only one sporulation sequence is known. Diplokaryotic sporonts undergo meiosis and synchronous nuclear division forming sporogonial plasmodia with two, four and eight nuclei enclosed within a persistent sporophorous vesicle. Cytokinesis of sporogonial plasmodia results in the formation of eight uninucleate spores. Spores are oval, thick walled, have a lamellar polaroplast, a moderately sized posterior vacuole (posterosome) filled with a matrix of moderate electron density, and a gradually tapered polar filament.

4.3.1.2. Etymology. Named in recognition of the contributions of Theodore Andreadis to the biology of mosquito–parasitic microsporidia.

4.3.2. Andreanna caspii n. sp

4.3.2.1. Diagnosis. With characters of the genus. Episporontal space of early sporonts filled with a homogeneous accumulation of electron dense granular inclusions and ovoid vesicles of various dimensions, transforming into an interwoven matrix during the initial phase of sporogenesis. Spores measure $4.8 \pm 0.3 \times 3.1 \pm 0.4$ μm (fixed). Spore wall 260 μm thick; exospore irregular with two layers, 150–170 μm thick; endospore 90–100 μm thick. Anchoring disk well developed and contiguous with a lamellar polaroplast which occupies the anterior third of the spore and possess more narrow lamellae at the posterior end. Polar filament arranged in a single row of six coils ranging from 180 to 150 μm in diameter.

4.3.2.2. Site of host infection and pathology. Fat body tissue of larvae. Third and fourth instar larvae appear swollen with dull white masses within the thorax and abdomen. Death occurs during the fourth instar.

4.3.2.3. Transmission. Unknown

4.3.2.4. Type host. Ochlerotatus caspius (Pallas) (Diptera: Culicidae)

4.3.2.5. Type locality. A shallow temporary vernal pool near the village of Teguldet, Tomsk region, Western Siberia, Russia (57° 18′ 44′ pr N, 88° 9′ 46′ pr W).

4.3.2.6. Prevalence. A natural infection rate of 0.5% ($n = 1222$) was estimated among late instar larvae collected in mid-June.

4.3.2.7. Type material. Giemsa-stained slides of infected larval tissues and Epon-embedded material used in the ultrastructural studies are in the collection of A.V. Simakova, Tomsk State University, Russia. Frozen DNAs of the microsporidian and the host mosquito are available from T.G. Andreadis, The Connecticut Agricultural Experiment Station, New Haven, CT.

4.3.2.8. Gene sequences. The SSU rDNA sequence of the microsporidium, *A. caspii* has been deposited in the GenBank/EMBL database under Accession No. EU664450. The SSU rDNA sequence of the host mosquito, *Oc. caspius* has been deposited in the GenBank/EMBL database under Accession No. EU700339.

4.3.2.9. Etymology. The species name refers to the type host.

Acknowledgments

We are grateful to A.A. Miller (Tomsk State University) for assistance with the ultrastructural studies and to John Shepard (CAES) for technical assistance with the DNA sequencing. This investigation was supported in part by research grant RFBR # 07-04-00468 issued to AVS and US Department of Agriculture Grants 58-6615-1-218 and CONH00768 issued to TGA.

References

Andreadis, T.G., 1983. Life cycle and epizootiology of *Amblyospora* sp. (Microspora: Amblyosporidae) in the mosquito, *Aedes cantator*.. J. Protozool. 30, 509–518.
Andreadis, T.G., 2007. Microsporidian parasites of mosquitoes. In: Floore, T.G. (Ed.), Biorational Control of Mosquitoes, Bull. No. 7, vol. 23. Am. Mosq. Control Assoc., pp. 3–29.

Andreadis, T.G., Hall, D.W., 1979. Development, ultrastructure, and mode of transmission of *Amblyospora* sp. (Microspora: Thelohaniidae) in the mosquito.. J. Protozool. 26, 444–452.

Andreadis, T.G., Vossbrinck, C.F., 2002. Life cycle, ultrastructure and molecular phylogeny of *Hyalinocysta chapmani* (Microsporidia: Thelohaniidae) a parasite of *Culiseta melanura* (Diptera: Culicidae) and *Orthocyclops modestus* (Copepoda: Cyclopidae). J. Eukaryot. Microbiol. 49, 350–364.

Becnel, J.J., Fukuda, T., 1991. Ultrastructure of *Culicosporella lunata* (Microsporida: Culicosporellidae fam. n.) in the mosquito *Culex pilosis* (Diptera: Culicidae) with new information on the developmental cycle. Europ. J. Protistol. 26, 319–329.

Becnel, J.J., Sweeney, A.W., 1990. *Amblyospora trinus* N Sp. (Microsporida: Amblyosporidae) in the Australian mosquito Culex halifaxi (Diptera: Culicidae). J. Protozool. 37, 584–592.

Becnel, J.J., Sprague, V., Fukuda, T., Hazard, E.I., 1989. Development of *Edhazardia aedis* (Kudo, 1930) n g., n. comb. (Microsporida: Amblyosporidae) in the mosquito *Aedes aegypti* (L.) (Diptera: Culicidae). J. Protozool. 36, 19–130.

Canning, E.U., Vavra, J., 2000. Phylum Microsporidia Balbiani, 1882. In: Lee, J.J., Leedale, G.F., Bradbury, P. (Eds.), An Illustrated Guide to the Protozoa, second ed. vol. 1. Society of Protozoologists, Lawrence, KS, pp. 39–126.

Chen, W.J., Kuo, T.L., Wu, S.T., 1998. Development of a new microsporidian parasite, *Intrapredatorus barri* n.g., n.sp. (Microsporida: Amblyosporidae) from the predacious mosquito *Culex fuscanus* Wiedemann (Diptera: Culicidae). Parasitol. Int. 47, 183–193.

Franzen, C., Nassonova, E.S., Scholmerich, J., Issi, I.V., 2006. Transfer of the genus *Brachiola* (Microsporidia) to the genus *Anncaliia* based on ultrastructural and molecular data *L.*. J. Eukaryot. Microbiol. 53, 26–35.

Gucevich, A.V., Monchadskiy, A.S., Shtakelberg, A.S., 1970. Mosquitoes family Culicidae. Insects Diptera. Fauna of USSR 3, 184–314 (in Russian).

Kilochitskii, P.J., 1997. Two new microsporidian Genera: *Aedispora* gen. n. (Culicosporida, Culicosporidae) and *Krishtalia* gen. n. (Culicosporida, Golbergiidae) of the blood sucking mosquitoes from the Ukraine. Vestnik Zoologii 31, 15–23 (in Russian with English summary).

Kilochitskii, P.J., 2002. Microsporidia of the Blood Sucking Mosquitoes, Kiev, Geoprint (in Ukrainian).

Larsson, J.I.R., 1988. Identification of microsporidian genera (Protozoa, Microspora) – a guide with comments on taxonomy. Arch. Protistenkd. 136, 1–37.

Larsson, J.I.R., 1999. Identification of microsporidia. Acta Protozool. 38, 161–197.

Larsson, R., 1986. Ultrastructure, function, and classification of microsporidia. Progr. Protistol. 1, 325–390.

Lukes, J., Vavra, J., 1990. Life cycle of *Amblyospora weiseri* n.sp.: (Microsporidia) in *Aedes cantans* (Diptera, Culicidae). Europ. J. Protistol. 25, 200–208.

Micieli, M.V., Garcia, J.J., Becnel, J.J., 2000. Life cycle and description of *Amblyospora camposi* n. sp. (Microsporidia: Amblyosporidae) in the mosquito *Culex renatoi* (Diptera: Culicidae) and the copepod *Paracyclops fimbriatus fimbriatus* (Copepoda: Cyclopidae). J. Eukaryot. Microbiol. 47, 575–580.

Nilsen, F., Chen, W.J., 2001. rDNA phylogeny of *Intrapredatorus barri* (Microsporida: Amblyosporidae) parasitic to *Culex fuscanus Wiedman* (Diptera: Culicidae). Parasitology 122, 617–623.

Pankova, T.F., Issi, I.V., Simakova, S.V., 2000. New species of *microsporidians Amblyospora* from blood-sucking mosquitos of the family Culicidae. Parazitologiya 34, 420–427 (in Russian with English summary).

Shepard, J.J., Andreadis, T.G., Vossbrinck, C.R., 2006. Molecular phylogeny and evolutionary relationships among mosquitoes (Diptera: Culicidae) from the northeastern United States based on small subunit ribosomal DNA (18S rDNA) sequences. J. Med. Entomol. 4, 443–454.

Sprague, V., Becnel, J.J., Hazard, E.I., 1992. Taxonomy of phylum Microspora. Crit. Rev. Microbiol. 18, 285–395.

Sweeney, A.W., Graham, M.F., Hazard, E.I., 1988. Life cycle of *Amblyospora dyxenoides* sp. nov. in the mosquito, *Culex annulirostris* and the copepod *Mesocyclops albicans*. J. Invertebr. Pathol. 51, 46–57.

Swofford, D.L., 1998. PAUP* Phylogenetic Analysis Using Parsimony and Other Methods. V. 4.0 Beta. Sinauer associates, Sunderland, MA. http://paup.csit.fsu.edu/Cmd_ref_v2.pdf.

Thompson, J.D., Gibson, T.J., Plewniak, F., Jeanmougin, F., Higgins, D.G., 1997. The ClustalX windows interface: flexible strategies for multiple sequence alignment aided by quality analysis tools. Nucleic Acids Res. 24, 4876–4882.

Vossbrinck, C.R., Debrunner-Vossbrinck, B.A., 2005. Molecular phylogeny of the microsporidia: ecological, ultrastructural and taxonomic considerations. Folia Parasitologica 52, 131–142.

Vossbrinck, C.R., Andreadis, T.G., Debrunner-Vossbrinck, B.A., 1998. Verification of intermediate hosts in the life cycles of microsporidia by small subunit rDNA sequencing. J. Eukaryot. Microbiol. 45, 290–292.

Vossbrinck, C.R., Andreadis, T.G., Vavra, J., Becnel, J.J., 2004. Molecular phylogeny and evolution of mosquito parasitic Microsporidia (Microsporidia: Amblyosporidae). J. Eukaryot. Microbiol. 51, 88–95.